Size Threshold in the Dibenzothiophene Adsorption on MoS_2 Nanoclusters

Anders Tuxen,[†] Jakob Kibsgaard,[†] Henrik Gøbel,[†] Erik Lægsgaard,[†] Henrik Topsøe,[‡] Jeppe V. Lauritsen,[†] and Flemming Besenbacher[†,*]

[†]Interdisciplinary Nanoscience Center (iNANO), and Department of Physics and Astronomy, Aarhus University, DK-8000 Aarhus C, Denmark, and [‡]Haldor Topsøe A/S, Nymøllevej 55, DK-2800 Kgs. Lyngby, Denmark

ABSTRACT In hydrodesulfurization (HDS) of fossil fuels, the sulfur levels are reduced by sulfur extraction from hydrocarbons through a series of catalyzed reaction steps on low-coordinated sites on molybdenum disulfide (MoS_2) nanoclusters. By means of scanning tunneling microscopy (STM), we show that the adsorption properties of MoS_2 nanoclusters toward the HDS refractory dibenzothiophene (DBT) vary dramatically with small changes in the cluster size. STM images reveal that MoS_2 nanoclusters with a size above a threshold value of 1.5 nm react with hydrogen to form so-called sulfur vacancies predominately located at edge sites, but these edge vacancies are not capable of binding DBT directly. In contrast, MoS_2 nanoclusters below the threshold perform remarkably better. Here, sulfur vacancies form predominantly at the corner sites, and these vacancies show a high affinity for DBT. The results thus indicate that very small MoS_2 nanoclusters may have unique catalytic properties for the production of clean fuels.

KEYWORDS: molybdenum disulfide (MoS_2) · hydrodesulfurization (HDS) · scanning tunneling microscopy (STM) · catalysis · nanocluster · size-dependent properties

Detailed control of the size of nanoparticles offers new possibilities for the design of materials with novel functional properties, such as new heterogeneous catalysts with unprecedented reactivity and selectivity.[1,2] The intrinsic size-dependent property of nanoclusters originates from the changes in the electronic structure induced by the spatial confinement of electrons within very small nanoclusters, and they may be manifested in terms of distinct functional changes in, for example, optical, magnetic, or electronic properties.[3] Size-dependent *catalytic* properties are, however, significantly more subtle in nature since typically only the surface atoms on the nanocluster are active. Superimposed on the intrinsic size-dependent electronic structure, one thus has the effect of low-dimensional surface defects such as step edges, kinks, corners, and atomic vacancies, which may induce additional local effects. Indeed, in catalysis, low-coordinated sites can be orders of magnitude more active than atoms on extended facets,[4−6] and more importantly, the catalytic selectivity for the reactants may be entirely different on these sites.[7,8] An important aspect of improving the catalytic activity and selectivity is thus to control the type of low-coordinated sites exposed on the surface of the nanoclusters.[9,10] The chemistry of such low-coordinated sites and defect sites is, however, poorly understood from a fundamental point of view, mainly due to the very limited possibilities for characterizing and controlling the atomic-scale structure of such active sites on the surface of nanoclusters.

This is also the case for the single-layer MoS_2 nanoclusters which constitute the basic catalytically active phase in the environmentally and technologically important hydrodesulfurization (HDS) catalysts employed to remove sulfur from crude oil feedstocks to comply with the current strict ultralow sulfur standards for transportation fuels.[11,12] Typically, so-called sulfur vacancies formed by reacting off sulfur atoms at the edges of MoS_2 nanoclusters by hydrogen are considered to be the main active sites involved in the direct removal of sulfur in the HDS process, but due to lack of detailed atomic-scale insight into the structure of the MoS_2 nanoclusters, several important questions have remained unanswered regarding the location of the active sites and their chemical affinity in HDS reactions. Achieving ultralow sulfur fuels with a sulfur content lower than 10 ppm on an industrial scale has proven to be a very difficult task because the feedstock contains a number of very refractory S-containing molecules, which due to their low reactivity easily pass untreated into the final fuel product using the standard industrial HDS catalysts.[13,14] The most abundant of these refractory molecules belongs to the

*Address correspondence to fbe@inano.dk.

Received for review May 19, 2010 and accepted June 23, 2010.

Published online July 6, 2010.
10.1021/nn1011013

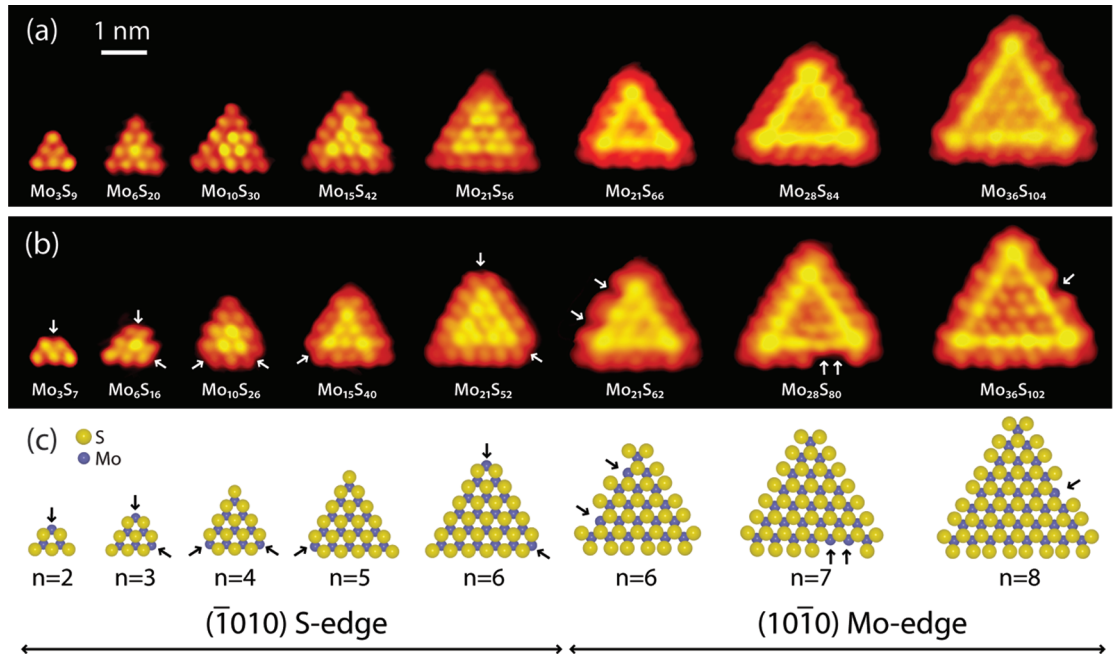

Figure 1. STM images of MoS_2 nanoclusters before and after exposure to atomic hydrogen. (a) MoS_2 nanoclusters before exposure to atomic hydrogen. Clusters with $n > 6$ expose the (10$\bar{1}$0) Mo edge termination, while clusters with $n < 6$ expose the ($\bar{1}$010) S edge termination. (b) MoS_2 nanoclusters with sizes similar to those in (a) but after exposure to atomic hydrogen at 300 K. The arrows indicate sulfur vacancies. (c) Ball models of the nanoclusters in (b).

dibenzothiophene (DBT) family, and the origin of the low reactivity of these molecules is attributed to sterical hindrance, which hinders the direct contact of the sulfur heteroatom with the active surface site needed to catalyze the C−S bond scission.[15] Here we use the unique capability of scanning tunneling microscopy (STM) to selectively probe and atomically resolve the active sites of MoS_2 nanoclusters.[16,17] We show that DBT molecules only bind to a particular type of low-coordinated corner vacancy sites on single-layer MoS_2 nanoclusters. Very interestingly, we find that the distinct nature and concentration of these binding sites vary significantly with the size of the nanoclusters; that is, both the probability to form S vacancy sites at the corners and their affinity for DBT chemisorptions is highest for nanoclusters with a size (edge length) smaller than a critical threshold size of 1.5 nm. The enhanced sulfur vacancy formation probability and the enhanced affinity for DBT binding at the corner sites of the very small clusters can be fully explained in terms of related changes in the edge termination of the MoS_2 nanoclusters.

RESULTS AND DISCUSSION

To explore the size-dependent adsorption properties of MoS_2, we have studied single-layer MoS_2 nanoclusters synthesized on the chemically inert single-crystal Au(111) substrate under well-controlled ultrahigh vacuum (UHV) conditions.[16] The characteristic "herringbone" reconstruction of Au(111) has previously been shown to act as a useful template to support the synthesis of an ensemble of single-layer MoS_2 nanoclusters with an extremely well-defined triangular equilibrium shape and a very reproducible and narrow size distribution.[18] Figure 1a depicts a series of atomically resolved STM images of the most prevalent of the MoS_2 nanoclusters and corresponding ball models reflecting the atomic-scale structure as previously determined by density functional theory (DFT)-based STM simulations of both extended MoS_2 slabs and finite size MoS_2 nanoclusters.[19,20] The MoS_2 nanoclusters in Figure 1a are arranged according to their size, which we represent in terms of the number (n) of Mo atoms along the edges of the triangular clusters.

As illustrated in Figure 1, the equilibrium edge structure of the MoS_2 nanoclusters depends on their size,[18] an effect which is reflected in the changes in the registry and coordination of S atoms on the cluster. All MoS_2 nanoclusters with $n > 6$ have been determined to be terminated by the fully sulfided (10$\bar{1}$0) Mo edges of MoS_2.[18] The main STM signature of these S-terminated Mo edges is the out of registry positioning of the outermost row of protrusions relative to the sulfur lattice of the basal plane of the MoS_2 nanoclusters and a ~0.4 Å high bright brim located adjacent to the outermost row of protrusions in Figure 1a.[21] This bright brim reflects a one-dimensional (1D) metallic edge state pertaining to this particular edge termination of a single MoS_2 layer.[21] For MoS_2 triangles with $n < 6$, a brim is no longer resolved in the STM images, and the outermost row of protrusions is now instead located in registry with the basal plane sulfur lattice. This shift in structural appearance reflects a change of the equilibrium termination of the MoS_2 nanoclusters from a fully S -terminated

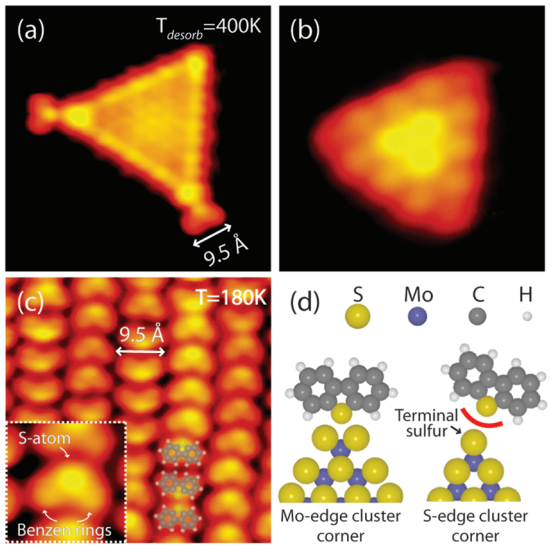

Figure 2. Adsorption of dibenzothiophene (DBT). (a) STM image (52 × 52 Å^2) of a Mo-edge-terminated cluster after dosing of DBT at 300 K. (b) S-edge-terminated cluster after dosing of DBT at 300 K. The image is 22 × 22 Å^2. (c) DBT molecules on the virgin Au(111) surface at 180 K. The image is 50 × 50 Å^2. The inset shows a close-up STM image (15 × 15 Å^2) of a DBT molecule. (d) Illustrations of the adsorption of DBT on the corner sites of Mo- and S-edge-terminated clusters.

$(10\bar{1}0)$ Mo edge to a $(\bar{1}010)$ S edge termination as the cluster size is reduced. Nanoclusters with exactly $n = 6$ represent a bistable situation, where both the $(10\bar{1}0)$ Mo edge and $(\bar{1}010)$ S edge termination are observed with almost equal probability (Figure 1a). This structural transition as the clusters become smaller is explained by the S:Mo stoichiometry of the entire cluster, which increases sharply as the nanocluster size is reduced due to the excess amount of sulfur saturating the cluster edges.[18] The observed structural transformation at $n = 6$ coincides with the point where the total S:Mo ratio for the Mo-edge-terminated nanoclusters exceeds a critical value of 3, above which the Mo-edge-terminated MoS_2 nanoclusters are no longer stable. For MoS_2 nanoclusters with $n = 6$, this S:Mo value can be reduced below 3 again by structural transition to S-edge-terminated MoS_2 nanoclusters, and accordingly, all of the smallest clusters adopt a S-edge-terminated structure. As depicted in the ball models in Figure 1c, the smallest MoS_2 nanoclusters expose edges which are structurally different, and these small clusters are therefore likely to have very different adsorptive and catalytic properties. We note that a direct transformation between the two different edge structures cannot be obtained by simple adsorption/desorption events of single sulfur atoms.

To explore how the catalytic properties vary with the cluster size, we expose the freshly synthesized nanoclusters to DBT vapor (see Methods) and, subsequently, systematically map the preferential adsorption sites of DBT on the clusters in STM images. Figure 2a depicts an atom-resolved STM image of a large $n = 10$ MoS_2 nanocluster after exposure to DBT at room temperature. Interestingly, the DBT molecules are observed to be adsorbed on two of the corner sites, while no molecules are observed to adsorb on edge sites or on top of the nanoclusters under these conditions. The size of the molecules adsorbed on the corner sites is determined to be ~9.5 Å, which is in very good agreement with the expected size of a DBT molecule.[22] The symmetry of the adsorbed DBT molecules in the STM image indicates a flat adsorption geometry of the DBT molecules on the Au(111) surface with the S atom pointing toward the corner of the cluster. This flat lying adsorption configuration of the DBT molecules is supported by the STM images in Figure 2c recorded on a self-assembled monolayer of DBT molecules, which forms on the bare Au(111) at a lower temperature of 180 K. The inset in this figure reveals that each molecule in this structure is imaged with a bright protrusion on one side and two slightly fainter protrusions on the opposite side. In view of the molecular structure of DBT, these results suggest that the bright protrusion stems from the sulfur atom in the thiophene ring while the two fainter protrusions arise from the benzene rings. The image depicted in Figure 2a thus suggests very interestingly that the DBT molecules at room temperature preferentially adsorb at the corner sites of the fully sulfided clusters *via* the sulfur atom. However, it should be noted that the interaction between the Mo edge corner sites and the DBT molecules is rather weak since upon annealing to ~400 K the DBT molecules desorb from these corner sites. Adsorption of DBT was also investigated on the smallest MoS_2 nanoclusters with the S edge termination. For these clusters, we find that the molecule cluster interaction is even weaker because no adsorption of DBT is observed at room temperature on these fully sulfided clusters, as illustrated in Figure 2b for a $n = 4$ triangle after exposure to DBT at room temperature. We attribute this difference in the DBT adsorption behavior of the two MoS_2 nanoclusters to the difference between the structures of the corner sites on the two types of clusters. The corner sites of the small S-edge-terminated cluster have terminal sulfur atoms on the corner sites, which apparently prevent interaction between the nanocluster and the sulfur atom in the DBT molecule (Figure 2d). This situation is quite different from that encountered at the corner sites of the larger Mo edge clusters (Figure 2d), where the sulfur atoms are adjacent to the corner.

Under real HDS catalytic reaction conditions, the MoS_2 nanoclusters are exposed to a mixture of sulfur-containing molecules and hydrogen. We have therefore investigated how hydrogen influences the adsorption properties of the MoS_2 nanoclusters. One way hydrogen can modify the atomic-scale morphology of the nanoclusters is to react with surface sulfur atoms, yielding H_2S and leaving sulfur vacancies at the edges of the MoS_2 nanoclusters behind. To create these vacancies,

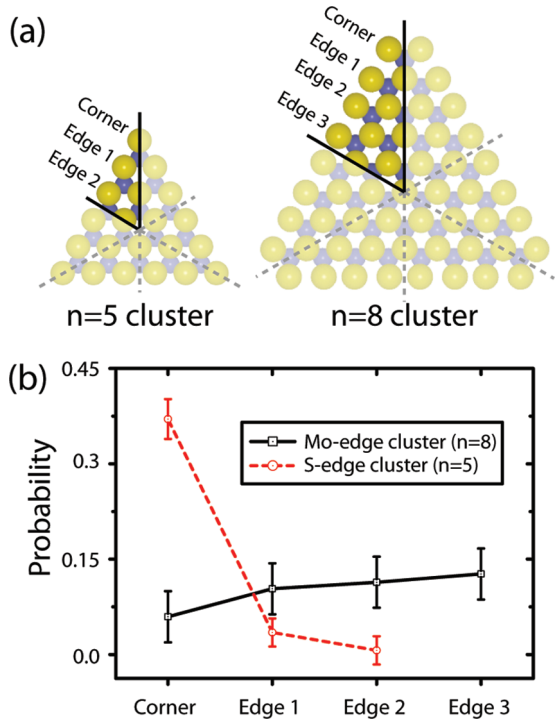

Figure 3. Statistical analysis of sulfur vacancies. (a) Definition of edge and corner sites on triangular $n = 5$ and $n = 8$ clusters. (b) Probability of vacancy formation on edge and corner sites on S edge ($n = 5$) cluster and Mo edge ($n = 8$) cluster. Error bars are calculated as one over the square root of the number of evaluated sites (see Supporting Information for details).

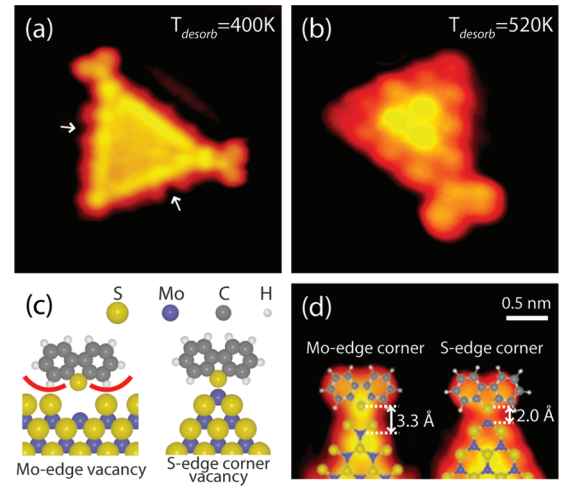

Figure 4. Adsorption of DBT on MoS_2 nanoclusters after exposure to atomic hydrogen. (a) Large ($n = 10$) Mo-edge-terminated nanocluster after exposure to atomic hydrogen and DBT (56 × 56 Å^2). (b) Small ($n = 4$) S-edge-terminated nanocluster after exposure to atomic hydrogen and DBT (25 × 25 Å^2). (c) DBT adsorption configurations on edge and corner vacancies on Mo edge and S edge clusters, respectively. (d) High-resolution STM images of DBT molecules on corner sites with the adsorption models superimposed on the STM images.

which may constitute additional adsorption sites, we pre-expose the MoS_2 nanoclusters to atomic H by predissociating H_2 on a hot W filament to the hot sample. This procedure is widely applied in ultrahigh vacuum (UHV) studies in order to expose samples to a high chemical potential of hydrogen similar to that encountered under high-pressure catalytic conditions.[16]

Figure 1b shows MoS_2 nanoclusters after exposure to atomic hydrogen, and from the atomically resolved STM images, it is clear that H exposure has led to the formation of sulfur vacancies on the MoS_2 clusters. The vacancies are identified as the missing protrusions on the clusters, and they are indicated by small arrows. From a detailed analysis of several STM images, we can conclude that the preferential position of the S vacancies varies significantly with the size of the MoS_2 nanoclusters. For the larger Mo-edge-terminated nanoclusters ($n \geq 6$), we observe that the sulfur vacancies preferentially form at the edges (see Figure 1b to the right). This is in distinct contrast to what is observed for the small S-edge-terminated nanoclusters ($n \leq 6$), for which we predominately observe vacancies on the corner sites (see Figure 1b to the left). In fact, all of the small clusters in Figure 1b only have vacancies at the corner sites. A thorough statistical analysis of many sulfur vacancies observed on $n = 5$ and $n = 8$ MoS_2 nanoclusters, which are the most abundant "small" and "large" clusters, respectively, fully confirms this qualitative picture (Figure 3b). For the small $n = 5$ clusters, the analysis reveals the preference for corner vacancies, and the probability of formation of S vacancies at the edges is small. For the large $n = 8$ nanocluster, the behavior appears to be opposite. Here, the vacancies preferentially form at the edges, and the sulfur vacancy probability actually drops the closer the site is to the corner of the cluster.

We have subsequently dosed DBT molecules to the nanoclusters pre-exposed to atomic hydrogen to reveal the adsorption properties of nanoclusters containing sulfur vacancies. In Figure 4a, we show the result of a large Mo-edge-terminated nanocluster ($n = 10$) imaged at room temperature. For these clusters, hydrogen activation leads to the creation of edge vacancies, and it is remarkable that this nanocluster still exhibits two edge sulfur vacancies (marked by white arrows in Figure 4a) after exposure to DBT. The finding that no adsorption of DBT molecules is observed on the edge vacancies is very interesting from a hydrotreating catalytic point of view because it shows that sterical hindrance prevents adsorption of DBT on edge vacancies on the larger MoS_2 nanoclusters (Figure 4c), and such sites therefore most likely possess low catalytic HDS activity for the direct extrusion of S from DBT. The only adsorption configuration that we observe on the large Mo edge clusters is the corner absorbed DBT molecules, which we also identified prior to hydrogen activation. The DBT molecules adsorbed at these corner sites do not appear to be affected by the hydrogen activation because sulfur vacancy formation here is less favored (Figure 3b). Indeed, desorption experiments show that the DBT molecules at the corner sites desorb at the

same temperature as before hydrogen activation, which indicates a weak physisorbed configuration. Moreover, by superimposing the structure of the nanocluster and the DBT molecule on the STM image depicted in Figure 4d, we find that the distance between the S atom in the molecule and the Mo atom on the corner site is 3.0 Å. This distance is quite large and indicates that there is no strong chemical interaction between the DBT molecule and the corner Mo atom in the nanocluster. The situation is markedly different for the smallest S-edge-terminated nanoclusters ($n < 6$), which preferentially form vacancies at the corner sites upon hydrogen exposure (Figure 3b). As revealed by the STM results in Figure 4b, these corner vacancy sites on the small nanoclusters bind DBT strongly. The fact that this adsorption configuration was *only* observed after the atomic hydrogen as seen from a comparison of Figure 2b and 4b suggests that DBT adsorption occurs on the sulfur vacancies induced by the atomic hydrogen exposure. Moreover, a thorough and detailed analysis of the STM image in Figure 4d shows that the observed adsorption configuration exactly matches a configuration where the DBT molecule adsorbs on the corner vacancy with the sulfur atom pointing toward the undercoordinated Mo atom protruding from the corner site. The observed distance between the Mo corner atom and the S atom in the DBT molecule is 2.0 Å, which is lower that the Mo−S distance in MoS_2 (~2.4 Å) and indicates a rather strong bonding between the DBT molecule and the Mo atom in the cluster. From a series of desorption experiments (see Supporting Information for details), we estimate the desorption temperature for this novel adsorption configuration to be around 520 K; that is, the DBT molecule is *chemisorbed* to the corner vacancies on these very small S-edge-terminated MoS_2 nanoclusters.

From an industrial catalysis point of view, the new STM insight into the adsorption selectivity of the different MoS_2 nanoclusters is very interesting because the results show that the steric constraints which prevent DBT adsorption on the ordinary edge S vacancies can be overcome on the unrestricted corner vacancy sites on very small ($n < 6$) MoS_2 nanoclusters. The adsorption of DBT molecules through the sulfur atom in the thiophene ring, referred to as a σ-adsorption,[23] has been considered to be a prerequisite for the direct route leading to sulfur extrusion, and our novel STM findings reveal that the corner sites are the most likely candidates as active sites for the direct desulfurization (DDS) of molecules such as DBT. In a second series of experiments, we have exposed the MoS_2 nanoclusters to the related and one of the most refractory S-containing molecules in crude oil, 4,6-dimethyldibenzothiophene (4,6-DMDBT). For this molecule, the DDS route is expected to be less favored than for DBT because the methyl groups in the 4 and 6 positions strongly hinder σ-adsorption through the S heteroatom.[15] In full accordance with this view, we find from our STM studies that 4,6-DMDBT never adsorbs on any of the sulfur vacancy configurations of the MoS_2 nanoclusters studied here, not even on the highly accessible corner vacancies on the small clusters.

CONCLUSIONS

By means of high resolution STM, we have revealed the adsorption properties of dibenzothiophene (DBT) and methyl-substituted DBT (4,6-DMDBT) on MoS_2 nanoclusters of different sizes. These results have provided new insights into the role of edge and corner sites as active sites in the important hydrodesulfurization reactions. Our results show very surprisingly that the adsorption properties depend in a striking way on the size of the MoS_2 nanoclusters, and that this size-dependent selectivity correlates with the size-related structural changes of the MoS_2 nanoclusters. Larger MoS_2 nanoclusters with more than 6 Mo atoms on the cluster edge show a preference for S vacancy formation on the edges, but these edge vacancies do not appear to have any affinity for binding DBT due to their sterical hindrance. However, smaller MoS_2 nanoclusters with less than the threshold value of 6 Mo atoms are found to form vacancies predominately on corners sites, and this is seen to be a favorable situation because the unconstrained access to Mo at such corner S vacancies sites enables strong adsorption of DBT molecules. Our results thus imply that corner sites on MoS_2 nanoclusters may play a hitherto unknown key role in the direct desulfurization of DBT and related molecules present in crude oil feedstocks, and that enhanced catalytic activity may be achieved by optimizing the number of the smallest MoS_2 nanoclusters in hydrodesulfurization catalysts. Similar special corner sites with size-dependent adsorption strength are envisioned to exist also in the optimized industrial type Ni- and Co-promoted MoS_2 hydrotreating catalysts,[24] and with detailed atomic-scale knowledge on such sites in hand, the prospects are that novel HDS catalysts with unprecedented activity and selectivity may be synthesized.

METHODS

Sample Preparation. All experiments were performed in a UHV chamber with a base pressure below 1×10^{-10} mbar. MoS_2 nanoclusters were synthesized by physical vapor deposition of molybdenum (Mo) in an atmosphere of 5×10^{-8} mbar H_2S until 10% of a monolayer was achieved. Subsequently, the sample was post-annealed to 673 K while the background pressure of H_2S was maintained. The details of the synthesis can be found in ref 25. The adsorption of DBT on MoS_2 nanoclusters was investigated by dosing dibenzothiophene (DBT) (Sigma-Aldrich, 98%

purity) to the synthesized MoS_2 nanoclusters in the UHV chamber. The DBT molecules were stored in a glass container and admitted to the UHV chamber through a leak valve. However, due the low vapor pressure of DBT, it was necessary to heat the gas line and the leak valve to the melting point of DBT (100 °C). DBT was typically dosed at a pressure of 5×10^{-9} mbar for about 30 s. The exact same procedure was used for the dosing of 4,6-dimethyldibenzothiophene (4,6-DMDBT) with the only difference being that the leak valve and gas line were heated to the melting point of 4,6-DMDBT (150 °C). Atomic hydrogen was produced by predissociating hydrogen on a very hot tungsten filament placed 15 cm from the sample and backfilling the UHV chamber with hydrogen to a pressure of 1×10^{-7} mbar. The dosing was maintained for 3 min while the sample temperature was kept at 400 K.

Scanning Tunneling Microscopy. All STM images were recorded on the high-stability Aarhus STM,[26] which is capable of achieving atomic resolution on a routine basis over a wide range of temperatures. All STM images were recorded in constant current mode with the sample held at a negative bias with respect to the tip. For all images, typical tunneling parameters were I_t = 0.5 nA and $V_t = -0.5$ V.

Acknowledgment. We would like to acknowledge stimulating discussions with Berit Hinnemann, Stig Helveg, Michael Brorson, and Kim G. Knudsen. We acknowledge the generous financial support from the Lundbeck Foundation, the Carlsberg Foundation, the Villum Kahn Rasmussen Foundation, the Danish Strategic Research Council (NABIIT Project 2106-06-0016), and Haldor Topsøe A/S. J.V.L. acknowledges support from the European Research Council (ERC) through a Starting Independent Researcher Grant (#239834, OxideSynergy). F.B. also acknowledges support from the European Research Council (ERC) for an Advanced Researcher Grant (#227430, VIN).

Supporting Information Available: Additional details and figures. This material is available free of charge *via* the Internet at http://pubs.acs.org.

REFERENCES AND NOTES

1. Valden, M.; Lai, X.; Goodman, D. W. Onset of Catalytic Activity of Gold Clusters on Titania with the Appearance of Nonmetallic Properties. *Science* **1999**, *281*, 1647–1650.
2. Haruta, M. Size- and Support-Dependency in the Catalysis of Gold. *Catal. Today* **1997**, *36*, 153–166.
3. Wang, Y.; Herron, N. Syntheses and Characterization of Nanometer-Sized Semiconductor Clusters. *Res. Chem. Intermed.* **1991**, *15*, 17–29.
4. Zambelli, T.; Wintterlin, J.; Trost, J.; Ertl, G. Identification of the "Active Sites" of a Surface-Catalyzed Reaction. *Science* **1996**, *273*, 1688–1690.
5. Dahl, S.; Logadottir, A.; Egeberg, R. C.; Larsen, J. H.; Chorkendorff, I.; Törnquist, E.; Nørskov, J. K. Role of Steps in N_2 Activation on Ru(0001). *Phys. Rev. Lett.* **1999**, *83*, 1814–1817.
6. Hammer, B. Bond Activation at Monatomic Steps: NO Dissociation at Corrugated Ru(0001). *Phys. Rev. Lett.* **1999**, *83*, 3681–3684.
7. Vang, R. T.; Honkala, K.; Dahl, S.; Vestergaard, E. K.; Schnadt, J.; Lægsgaard, E.; Clausen, B. S.; Nørskov, J. K.; Besenbacher, F. Controlling the Catalytic Bond Breaking Selectivity of Ni Surfaces by Step Blocking. *Nat. Mater.* **2005**, *4*, 160–163.
8. Lee, I.; Delbecq, F.; Morales, R.; Albiter, M. A.; Zaera, F. Tuning Selectivity in Catalysis by Controlling Particle Shape. *Nat. Mater.* **2009**, *8*, 132–138.
9. Tian, N.; Zhou, Z. Y.; Sun, S. G.; Ding, Y.; Wang, Z. L. Synthesis of Tetrahexahedral Platinum Nanocrystals with High-Index Facets and High Electro-Oxidation Activity. *Science* **2007**, *316*, 732–735.
10. Schmidt, E.; Vargas, A.; Mallat, T.; Baiker, A. Shape-Selective Enantioselective Hydrogenation on Pt Nanoparticles. *J. Am. Chem. Soc.* **2009**, *131*, 12358–12367.
11. Topsøe, H.; Clausen, B. S.; Massoth, F. E. *Hydrotreating Catalysis*; Springer Verlag: Berlin-Heidelberg, 1996; Vol. 11, p 459.
12. Prins, R. Hydrodesulfurization, Hydrodenitrogenation, Hydrodeoxygenation and Hydrodechlorination. In *Handbook of Heterogeneous Catalysis*; Ertl, G., Knözinger, H., Weitkamp, J., Eds.; VHC: Weinheim, Germany, 1997; Vol. 4, p 1908.
13. Topsøe, H.; Knudsen, K. G.; Byskov, L. S.; Nørskov, J. K.; Clausen, B. S. Advances in Deep Desulfurization. *Stud. Surf. Sci. Catal.* **1999**, *121*, 13–22.
14. Song, C. An Overview of New Approaches to Deep Desulfurization for Ultra-Clean Gasoline, Diesel Fuel and Jet Fuel. *Catal. Today* **2003**, *86*, 211–263.
15. Egorova, M.; Prins, R. Hydrodesulfurization of Dibenzothiophene and 4,6-Dimethyldibenzothiophene over Sulfided NiMo/γ-Al_2O_3, CoMo/γ-Al_2O_3, and Mo/γ-Al_2O_3. *J. Catal.* **2004**, *225*, 417–427.
16. Lauritsen, J. V.; Besenbacher, F. Model Catalyst Surfaces Investigated by Scanning Tunneling Microscopy. *Adv. Catal.* **2006**, *50*, 97–143.
17. Kushmerick, J. G.; Kandel, S. A.; Han, P.; Johnson, J. A.; Weiss, P. S. Atomic-Scale Insights into Hydrodesulfurization. *J. Phys. Chem. B* **2000**, *104*, 2980–2988.
18. Lauritsen, J. V.; Kibsgaard, J.; Helveg, S.; Topsøe, H.; Clausen, B. S.; Besenbacher, F. Size-Dependent Structure of MoS_2 Nanocrystals. *Nat. Nanotechnol.* **2007**, *2*, 53–58.
19. Bollinger, M. V.; Jacobsen, K. W.; Nørskov, J. K. Atomic and Electronic Structure of MoS_2 Nanoparticles. *Phys. Rev. B* **2003**, *67*, 085410.
20. Li, T. S.; Galli, G. L. Electronic Properties of MoS_2 Nanoparticles. *J. Phys. Chem. C* **2007**, *111*, 16192–16196.
21. Bollinger, M. V.; Lauritsen, J. V.; Jacobsen, K. W.; Nørskov, J. K.; Helveg, S.; Besenbacher, F. One-Dimensional Metallic Edge States in MoS_2. *Phys. Rev. Lett.* **2001**, *87*, 196803.
22. The distance between the hydrogen atoms protruding on each side of the DBT molecule is 9.6 Å.
23. Egorova, M.; Prins, R. The Role of Ni and Co Promoters in the Simultaneous HDS of Dibenzothiophene and HDN of Amines over Mo/γ-Al_2O_3 Catalysts. *J. Catal.* **2006**, *241*, 162–172.
24. Lauritsen, J. V.; *et al.* Location and Coordination of Promoter Atoms in Co- and Ni-Promoted MoS_2-Based Hydrotreating Catalysts. *J. Catal.* **2007**, *249*, 220–233.
25. Helveg, S.; Lauritsen, J. V.; Lægsgaard, E.; Stensgaard, I.; Nørskov, J. K.; Clausen, B. S.; Topsøe, H.; Besenbacher, F. Atomic-Scale Structure of Single-Layer MoS_2 Nanoclusters. *Phys. Rev. Lett.* **2000**, *84*, 951–954.
26. Lægsgaard, E.; Besenbacher, F.; Mortensen, K.; Stensgaard, I. A Fully Automated, Thimble-Size Scanning Tunnelling Microscope. *J. Microsc.* **1988**, *152*, 663–669.